Coronal mass ejections and magnetic flux buildup in the heliosphere

M. J. Owens[1] and N. U. Crooker[1]

[1] To test for magnetic flux buildup in the heliosphere from coronal mass ejections (CMEs), we simulate heliospheric flux as a constant background open flux with a time-varying interplanetary CME (ICME) contribution. As flux carried by ejecta can only contribute to the heliospheric flux budget while it remains closed, the ICME flux opening rate is an important factor. Two separate forms for the ICME flux opening rate are considered: (1) constant and (2) exponentially decaying with time. Coronagraph observations are used to determine the CME occurrence rates, while in situ observations are used to estimate the magnetic flux content of a typical ICME. Both static equilibrium and dynamic simulations, using the constant and exponential ICME flux opening models, require flux opening timescales of $\sim$50 days in order to match the observed doubling in the magnetic field intensity at 1 AU over the solar cycle. Such timescales are equivalent to a change in the ICME closed flux of only $\sim$7–12% between 1 and 5 AU, consistent with CSE signatures; no flux buildup results. The dynamic simulation yields a solar cycle flux variation with high variability that matches the overall variability of the observed magnetic field intensity remarkably well, including the double peak forming the Gnevyshev gap.

Citation: Owens, M. J., and N. U. Crooker (2006), Coronal mass ejections and magnetic flux buildup in the heliosphere, *J. Geophys. Res.*, *111*, A10104, doi:10.1029/2006JA011641.

1. Introduction

[2] The total unsigned magnetic flux in the heliosphere, as inferred by both in situ spacecraft measurements [*Lockwood et al.*, 2004] and potential field solutions to the photospheric field [*Wang et al.*, 2000a], approximately doubles over the solar cycle. This large-scale variation in flux is not the result of the transient magnetic field enhancements associated with interplanetary coronal mass ejections (ICMEs) convecting over the observing spacecraft but appears to be carried by the background solar wind [*Richardson et al.*, 2002]. In this study, building upon the work of *Luhmann et al.* [1998] and *Crooker et al.* [2002], we investigate the possibility that the closed flux injected into the heliosphere by coronal mass ejections (CMEs) persists long after the recognizable ICME structure has passed 1 AU, which leads to a periodic buildup in the CME contribution to the heliospheric magnetic flux budget.

[3] Figure 1 shows the proposed evolution of the heliospheric flux in 4 stages. Solid black lines represent magnetic field lines/arrows and larger red arrows show the direction of the suprathermal electron heat flux. The first panel shows the preeruption heliospheric flux, which consists of the an open field line threading the source surface (the dashed curve). The closed field loop within the source surface does not contribute to the heliospheric total. In the second panel, the CME has erupted, and the resulting closed ICME loop now contributes to the total flux in the heliosphere and displays a counterstreaming suprathermal electron (CSE) signature due to both foot points being connected to the photosphere. By the third panel, near-Sun interchange reconnection has opened the closed ICME loop, changing the magnetic topology and removing the CSE signature. Finally, the last panel shows the newly reconfigured magnetic field. While the eruption has caused some restructuring of the solar field (the open field lines moving with respect to the closed loop), the total heliospheric flux has returned to its preeruption value.

[4] From Figure 1 it is clear that ICME flux can only contribute to the heliospheric flux budget as long as it remains closed. The connectivity of heliospheric magnetic flux can be inferred from in situ observations of the suprathermal election heat flux, with closed flux associated with counterstreaming electrons [*Gosling et al.*, 1987]. In situ observations of magnetic clouds [e.g., *Burlaga*, 1988], a subset of all ICMEs, between 1 and 5 AU suggest approximately 50–60% of the ICME flux remains closed out to 5 AU (thus continuing to add to the total heliospheric flux content) and that little evolution occurs during this stage of ICME propagation [*Shodhan et al.*, 2000; *Crooker et al.*, 2004; *Riley et al.*, 2004]. Hence *Crooker et al.* [2004] and *Riley et al.* [2004] concluded that ICMEs open over very long timescales (months to years). Such long time scales for ICME flux opening (IFO) mean a significant fraction of the ICME flux must remain closed when the leading edge

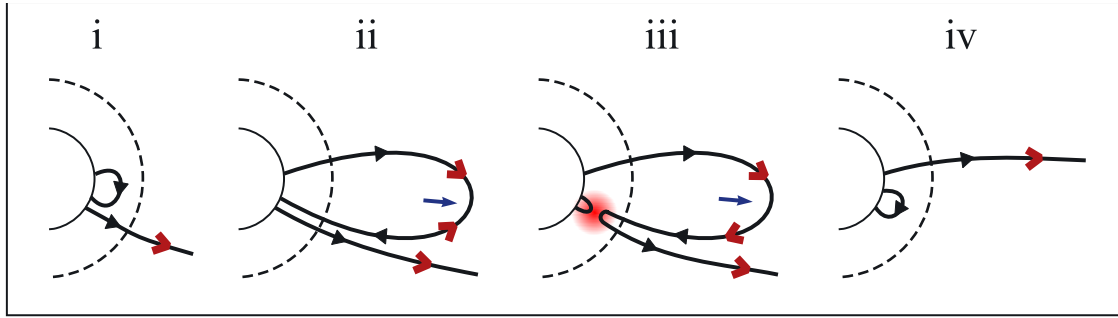[1]Center for Space Physics, Boston University, Boston, Massachusetts, USA.

Figure 1. A schematic representation of heliospheric magnetic flux evolution, with magnetic field lines shown as solid black lines/arrows and electron heat flux by larger red arrows. The dashed line curve represents a "source surface" beyond which magnetic field lines can contribute to the total heliospheric flux. (i) The preeruption heliospheric flux; (ii) posteruption, the closed ICME loop adds to the heliospheric total; (iii) interchange reconnection opens the closed ICME field line; (iv) the heliospheric flux returns to its pre-eruption value. Note the counterstreaming of electrons on the closed ICME loop (ii), which is subsequently removed by interchange reconnection (iii).

reaches very large heliocentric distances (e.g., >50 AU). It is assumed that the suprathermal electron strahl would scatter over such distances, removing the CSE signature at 1 AU. Thus the additional ICME magnetic flux would appear as ambient solar wind at 1 AU, in accord with the findings of *Richardson et al.* [2002].

[5] Using theoretical open field line diffusion rates, [*Reinard and Fisk*, 2004] proposed very fast ICME flux opening rates ($\sim$ hours), suggesting ICME fields should open rapidly beyond 1 AU. Additionally, it has been suggested that a buildup of heliospheric flux (the "flux catastrophe" [*McComas et al.*, 1992]) can only be avoided if ICME closed flux is very short lived ($\sim$ minutes). It should be noted if such fast IFO rates are correct, CSEs must exist on open magnetic field lines, calling into question the validity of a large body of research that uses suprathermal electrons as sensors of magnetic topology. In this study we will attempt to show that long ICME flux opening times do not result in a "flux catastrophe," and the use of CSEs as proxies for closed magnetic flux, at least out to 5 AU, need not be abandoned on the basis of the heliospheric flux budget.

2. Static Flux Equilibrium

[6] It is instructive to begin with a simple static equilibrium estimate of the ICME flux opening (IFO) rate required to match observations. As the radial component of the magnetic field (B_R) is constant with latitude, both at solar minimum and maximum [*Smith and Balogh*, 2003], near-Earth measurements can be used to estimate the total unsigned flux (Φ_T) in the heliosphere [*Lockwood et al.*, 2004]:

$$\Phi_T = 4\pi(1AU)^2|B_R| \approx 4\pi(1AU)^2|\mathbf{B}|\cos(45°). \quad (1)$$

We use $|\mathbf{B}|$ as a proxy for the total flux rather than $|B_R|$, as it eliminates averaging effects (i.e., changes in the polarity of B_R occurring within the 1-hour period of the observational averages used).

[7] The total heliospheric flux is assumed to consist of two components: a constant, background open flux, Φ_0, and a CME contribution, Φ_{CME}, which is the ICME closed flux summed over all the ICMEs in the heliosphere. We consider two simple IFO models: (1) the closed flux in an ICME, ϕ_C, opens at a constant rate (i.e., $d\phi_C = kdt$ where k is a constant [*Reinard and Fisk*, 2004]), and (2) the closed flux decays (i.e., opens) at a rate proportional to the amount of closed flux (i.e., $d\phi_C = -\lambda\phi_C \, dt$, where λ is the decay constant), giving an exponential IFO rate. The formulations are

$$\Phi_T = \Phi_0 + 2\sum_{n=1}^{N}[(1-D_n)\phi_n - k_n t_n]$$

$$\Phi_T = \Phi_0 + 2\sum_{n=1}^{\infty}[(1-D_n)\phi_n \exp(-\lambda_n t_n)], \quad (2)$$

where t_n is the lifetime of the nth ICME, ϕ_n is its total (closed and open) magnetic flux content and D_n is the fraction of that flux that opened at launch; λ_n and k_n are the two decay constants. For the constant IFO model, N is the number of the first completely open ICME (i.e., the first ICME for which $k_n t_n \geq (1-D)\phi$). Note the factor of two in the CME flux contribution, due to the closed CME loops intersecting a heliocentric sphere twice. As the properties of each individual event cannot be measured, it is necessary to assume that ϕ_n, D_n, λ_n and k_n can be represented by average values (ϕ, D, λ and k).

[8] If we assume the timescales involved are long enough that the heliospheric flux can be considered to evolve as a series of static equilibrium states, the CME occurrence rate (f) can be considered constant when calculating the instantaneous value of Φ_T. Thus the time between consecutive CMEs can be expressed as $1/f$, and the first completely open ICME will correspond to $N \geq f(1-D)\phi/k$. The total heliospheric flux contribution from ICMEs can then be expressed as

$$\Phi_{CME} = 2\sum_{n=1}^{N}\left[(1-D)\phi - \frac{nk}{f}\right]$$

$$\Phi_{CME} = 2(1-D)\phi\sum_{n=1}^{\infty}\left[\exp\left(\frac{-n\lambda}{f}\right)\right] = (1-D)\phi\coth\left(\frac{-\lambda}{2f}\right). \quad (3)$$

Table 1. Observational Estimates for the Parameters of the Heliospheric Flux Budget Calculation

Parameter	Symbol	Value
Average solar maximum $|\mathbf{B}|$ at 1 AU	$|\mathbf{B}_{MAX}|$	8 nT
Average solar minimum $|\mathbf{B}|$ at 1 AU	$|\mathbf{B}_{MIN}|$	5 nT
Average solar maximum CME rate	f_{MAX}	4 day^{-1}
Average solar minimum CME rate	f_{MIN}	1/3 day^{-1}
Typical axial flux in an ICME	ϕ	3 × 10^{12} Wb
Typical fraction of ϕ that opens at launch	D	0.5

Solving equations (1), (2), and (3) for flux equilibria attained at both solar minimum and solar maximum conditions and assuming the non-CME flux contribution, Φ_0, to be constant (i.e., all heliospheric flux variation can be attributed to CMEs) yields the following expressions for the expected heliospheric flux variation between solar minimum and solar maximum:

$$4\pi(1AU)^2(|\mathbf{B}_{MAX}| - |\mathbf{B}_{MIN}|)\cos\left(\frac{\pi}{4}\right) = \frac{(1-D)^2\phi^2(f_{MAX} - f_{MIN})}{k}$$

$$4\pi(1AU)^2(|\mathbf{B}_{MAX}| - |\mathbf{B}_{MIN}|)\cos\left(\frac{\pi}{4}\right)$$
$$= (1-D)\phi\left[\coth\left(\frac{\lambda}{2f_{MAX}}\right) - \coth\left(\frac{\lambda}{2f_{MIN}}\right)\right]. \quad (4)$$

[9] Typical values for the solar minimum and maximum CME frequency, f, are 1/3 and 4 day^{-1} [e.g., *Yashiro et al.* 2004] (see also Figure 4). We note that the LASCO-derived CME rate actually represents a lower limit to the true CME rate, with small, disc-centered CMEs being particularly difficult to observe with coronagraphs [*Yashiro et al.*, 2005]. However, as missed CMEs are likely to be significantly smaller than average they are likely to have a minimal effect on the total heliospheric flux budget. The 1 AU magnetic field intensity typically varies from ~5 to 8 nT [e.g., *Richardson et al.* 2002] (see also Figure 3). *Shodhan et al.* [2000], *Crooker et al.* [2004], and *Riley et al.* [2004] found D to be ~50%.

[10] The observational estimate for ϕ is the most uncertain of the required parameters. *Lynch et al.* [2005] fitted 132 magnetic clouds at 1 AU with a constant-α force-free magnetic flux rope model [*Burlaga*, 1988] and found a median axial flux content of 3 × 10^{12} Wb (only the closed axial component of a flux rope field can contribute to total heliospheric flux). As a circular cross section is assumed when fitting this flux rope model and elongated cross sections are more realistic [e.g., *Riley and Crooker*, 2004; *Owens et al.*, 2006], the total flux content of a magnetic cloud is probably somewhat underestimated by this method. Balancing this underestimate, however, is the fact that the axial field is concentrated in the core of the magnetic cloud and that the flux-rope structure may only represent a fraction of the total ICME structure [*Crooker et al.*, 1998]. Furthermore, the [*Burlaga*, 1988] approach to magnetic cloud modeling does not account for expansion as the flux rope convects over the spacecraft, which leads to an overestimation of the cloud radius and hence flux content. Finally, we note that using the *Lynch et al.* [2005] magnetic cloud estimate as an average for all ICMEs could be an overestimate because magnetic clouds amenable to fitting by a flux rope model at 1 AU probably represent a population of ICMEs with higher than average magnetic fluxes. Weaker flux ropes and/or nonflux rope structures may shred by interaction with the solar wind [*Cargill et al.*, 1996]. In spite of these caveats, the *Lynch et al.* [2005] estimate is in agreement with flux estimates of $\phi \sim 10^{12}$–10^{13} Wb from CME-associated coronal dimming regions, assumed to be the foot points of ejecta [e.g., *Webb et al.*, 2000].

[11] The observational estimates discussed above are listed in Table 1 and used for the quantities in equation (4). For the constant decay rate model in equation (4a), these values give a decay rate of $k = 1.3 \times 10^{10}$ Wb/day. This is equivalent to the posteruption ICME closed flux (i.e., $(1 - D)\phi$) halving in 55 days. We refer to this quantity as the "half-life," $T_{1/2}$. For the exponential decay rate model in equation (4b) the values in Table 1 yield a decay constant of $\lambda = 0.21$ s^{-1}, equivalent to a closed flux half-life, $T_{1/2}$, of ~38 days.

[12] To test whether these values for $T_{1/2}$ can explain the minimal change in the open ICME flux observed between 1 and 5 AU, Figure 2 shows the predicted change in ICME closed flux, $\Delta\phi_C$, for various flux opening times, for both the constant (dashed) and exponential (solid) IFO models. A constant ICME transit speed of 450 km/s was assumed (though very similar results are obtained for speeds in the range 300–600 km/s). Note that because only the percentage flux change is considered, this result is independent of the most uncertain parameter, the estimate of the typical ICME flux content (ϕ). The vertical lines show the static equilibrium calculated IFO times for the respective models: in both cases only a ~7–12% change is expected in the ICME closed flux, consistent with the value of ~5% inferred from observations [*Crooker et al.*, 2004; *Riley et al.*, 2004].

3. Dynamic Flux Simulation

[13] The CME rate continually changes over the solar cycle, and the timescales of the changes are comparable with IFO timescales (as calculated in section 2). Consequently, dynamic effects are likely to play a significant role in this problem. In this section we simulate the time-dependent variation of the heliospheric flux. Again we assume that the total heliospheric flux can be treated as two separate components (as per equation (1)). In the simulation, time is advanced in 0.1 day increments, and at each time step three actions are performed: (1) a check is made to see if a new ICME needs to be inserted into the heliosphere, (2) the heliospheric flux contribution from existing ICMEs is decayed using either the constant of exponential IFO model, and (3) the heliospheric flux is computed from summing the background open flux and the contribution from each ICME. The simulation is initialised by inserting CMEs at a rate of 0.5 per day for 2 years prior to the first LASCO observations [*Brueckner et al.*, 1995]. The main phase of the simulation begins where CMEs are inserted at the exact LASCO CME catalogue times [*Yashiro et al.*, 2004]. Again, we use the observed values of D and ϕ (0.5 and 3 × 10^{12} Wb, respectively). The value of Φ_0 is set
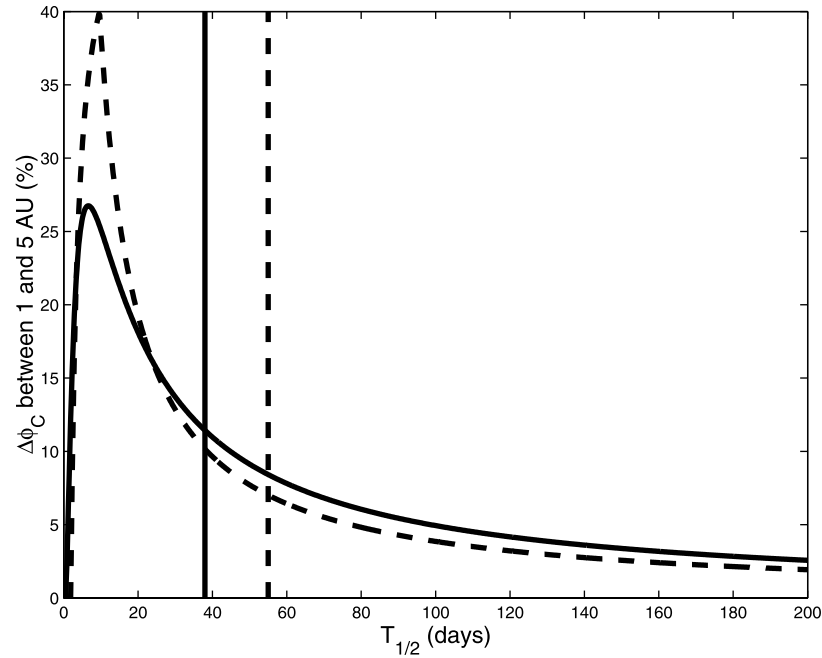
Figure 2. The predicted change in ICME closed flux (expressed as a percentage of the total ICME flux) between 1 and 5 AU, for the constant (dashed) and exponential (solid) IFO models. The vertical lines show the static equilibrium calculated IFO "half-lives" ($T_{1/2}$) for the respective models. This result is independent of the observational estimate for the average ICME flux (ϕ).

at 0.9×10^{15} Wb [e.g., *Wang et al.*, 2000a]. As only the flux variation is being modeled, however, the value of this constant background flux is unimportant.

[14] The red (blue) lines in Figure 3 show the simulated magnetic field intensities at 1 AU for the constant (exponential) IFO rate over a range of IFO half-lives: 1, 10, 25, **55**, and 100 days (1, 5, 25, **38**, and 70 days) for the constant

(exponential) IFO rate, with the smaller values of $T_{1/2}$ corresponding to the smaller values of $|\mathbf{B}|$, and thick colored lines correspond to the IFO half-lives in bold. The grey shaded regions show times when LASCO data were unavailable. (A nonphysical drop in the predicted 1 AU $|\mathbf{B}|$ during 1998 is addressed in section 4.) The black line shows the observed magnetic field intensity at 1 AU from the
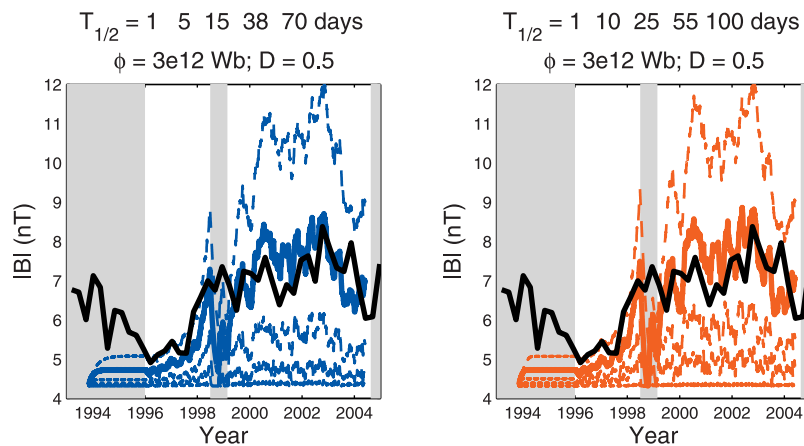

Figure 3. Simulations of heliospheric flux using the CME eruption times from the LASCO CME catalogue [*Yashiro et al.*, 2004]. Grey panels indicate times when LASCO observations were unavailable. The red (blue) plots show the simulated magnetic field intensity at 1 AU using the constant (exponential) IFO model for a range of IFO half-lives: 1, 10, 25, **55**, and 100 days (1, 5, 25, **38**, and 70 days) for the constant (exponential) IFO rate. Note that the smaller values of $T_{1/2}$ correspond to the smaller values of $|\mathbf{B}|$, and thick colored lines correspond to the IFO half-lives in bold. The solid black line shows the observed value of $|\mathbf{B_{1AU}}|$ (OMNI data).
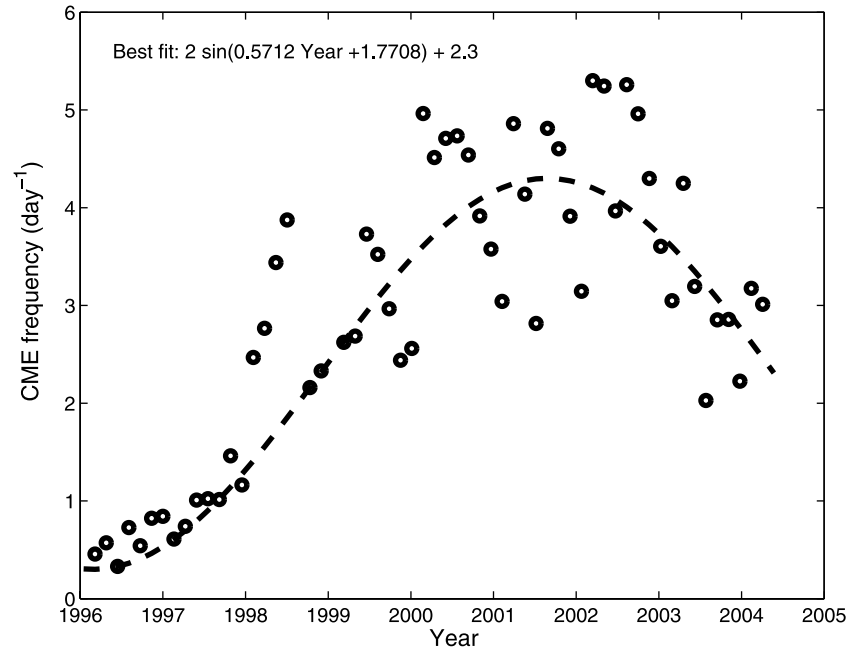
Figure 4. The observed LASCO CME frequency (50-day averaged with data gaps removed), and the best-fit sine-wave to the data (solid line).

National Space Science Center (OMNI) data, averaged over 100 days. This long time scale is required for the observed magnetic field strength to be representative of the heliospheric flux [*Lockwood et al.*, 2004].

[15] The most striking feature of Figure 3 is the match in the overall degree of variability between the simulated and observed solar cycle variations. In particular the maxima in 2000 and late 2002 on either side of the "Gnevyshev gap" (see below) match exactly. The observed amplitude variation in $|\mathbf{B}|$ at 1 AU is best matched by half-lives of $\sim$55 and 38 days for the constant and exponential IFO models, respectively, in agreement with the static equilibrium values calculated in section 2. For larger values of $T_{1/2}$ the predicted magnetic flux increases above that observed. Conversely, very small values of $T_{1/2}$ ($\leq$10 days) do not allow the ICME flux contribution to grow significantly and require a different mechanism to explain both the heliospheric flux variation and the CSE observations in ICMEs between 1 and 5 AU.

[16] Comparing the results from the two IFO models reveals little to separate them. It could be argued that for the optimal values of $T_{1/2}$ (55 days for the constant IFO model, 38 for the exponential), the constant IFO model better captures the Gnevyshev gap feature (i.e., the drop in the observed magnetic field intensity at 1 AU and CME frequency that occurs close to the peak of the solar cycle [*Gnevyshev*, 1977; *Richardson et al.*, 2002]), though in both models this feature is not as prominent as is observed. Conversely, the exponential model more accurately represents the asymmetry in $|\mathbf{B_{1AU}}|$ either side of the Gnevyshev gap. Note that with both IFO models the features of the Gnevyshev gap are more consistent with those observed when higher values of $T_{1/2}$ are used, though this also results in an overestimation of $|\mathbf{B_{1AU}}|$. Thus it is possible that simulations using longer IFO timescales in conjunction with

a smaller value of ϕ (which has a large observational uncertainty) would provide a better reconstruction of the observed heliospheric flux variation.

4. Multiple Solar Cycles

[17] In the simulation performed in section 3, gaps in the LASCO observations may have affected the predicted heliospheric flux. Furthermore, we want to determine the behavior of the CME flux contributions over more than one complete solar cycle to address the impact of long IFO times ($\sim$50 days) on a possible buildup of flux over multiple cycles. In this section we artificially construct CME times over multiple solar cycles using the LASCO observed CME frequencies of solar cycle 23.

[18] Figure 4 shows the 50-day averaged CME frequency (*f*) using the LASCO CME catalogue, with data gaps removed (periods where *f* dropped to zero were discounted from the averaging). As there is less than one complete cycle of data, it is necessary to make some assumptions about the form of *f*. We fit an 11-year periodic sine wave (for convenience, the CME dates are expressed in decimal year):

$$f\left(day^{-1}\right) = 2\sin\left[\frac{2\pi}{11}Year + 1.77\right] + 2.3. \qquad (5)$$

Assuming the CME rates and the length of the current solar cycle are representative of previous cycles, we use this observationally inferred CME rate to drive the heliospheric flux simulation over multiple solar cycles. Figure 5 shows the results. The red (blue) line shows the simulated value of $|\mathbf{B}|$ at 1 AU using the constant (exponential) IFO model with a $T_{1/2}$ of 55 (38) days. The solid black line shows the observed value of $|\mathbf{B_{1AU}}|$. It is clear that the simulations and
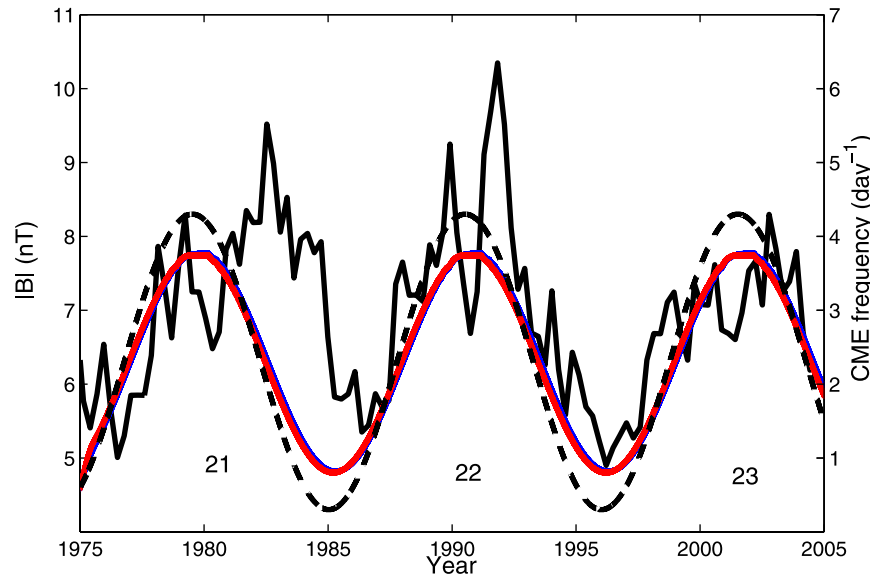
Figure 5. The simulated heliospheric flux driven by an 11-year periodic sine-wave fit to the LASCO observed CME frequency of solar cycle 23 (the dashed line and right hand axis. See also Figure 4). The red (blue) line shows the simulated value of $|\mathbf{B}|$ at 1 AU using the constant (exponential) model of IFO with a $T_{1/2}$ of 55 (38) days. The solid black line shows the observed value of $|\mathbf{B_{1AU}}|$.

observations are becoming out of phase by cycle 21, due to the fixed 11-year cycle length. Also, the peak of the magnetic flux in cycle 22 is much higher than in cycle 23, possibly due to an increased CME rate, which is obviously not captured using a fit to observations from a single cycle. Furthermore, any evidence of the Gnevyshev gap in the simulations has disappeared. Nevertheless, despite the relative simplicity of this driving CME function, there are still a number of important points to be derived from the results. Primarily, it is clear that for IFO times of ~50 days (in both the constant and exponential IFO rate models) there is no flux catastrophe. The heliospheric flux drops to the same value in consecutive solar cycles rather than continuously rising. Also, long IFO times may provide an explanation for the observed lag between the peaks of the CME frequency and $|\mathbf{B_{1AU}}|$. The simulation gives a lag of ~150 days. The observed lag is longer, however, again suggesting that a longer $T_{1/2}$ coupled with a smaller value for ϕ may be more appropriate, though the lack of the Gnevyshev gap in the driving CME frequency also contributes to this mismatch.

[19] As in section 3, there is not much to differentiate between the two IFO models. Though it is not readily apparent from Figure 5 (because of the long time-span considered), the heliospheric flux in the constant IFO rate model (red) rises and falls faster than in the exponential model (blue), despite the higher value of $T_{1/2}$ (55 compared to 38 days). Furthermore, the predicted $|\mathbf{B}|$ from the exponential model peaks both higher and later than the constant IFO model. These differences, however, are overwhelmed by the observational noise.

5. Discussion

[20] We have simulated the total heliospheric flux as an unchanging background open flux and a time-varying contribution from closed CME field lines. An observational estimate was used for the flux contribution from each CME, which was assumed to open either constantly or exponentially with time. Allowing the total flux to reach an approximate equilibrium at solar minimum and maximum requires ICME flux opening (IFO) half-lives between ~38 and 55 days. Use of LASCO CME observations to dynamically simulate the heliospheric flux yields a strikingly realistic solar cycle variation for similar IFO times. These values are equivalent to the ICME closed flux dropping by ~7–12% between 1 and 5 AU, consistent with the interpretation of counterstreaming electrons as signatures of closed ICME flux at these distances. In contrast, shorter IFO timescales of tens of days or less do not allow the CME flux contribution to build up sufficiently to match the observed solar cycle variation, and another mechanism is required. An additional simulation was performed using an 11-year periodic sine wave fit to the observed CME rates of solar cycle 23, allowing multiple solar cycles to be investigated. By using the typical force-free flux rope estimate of magnetic cloud flux as a proxy for the typical flux contained in all ICMEs, we are probably overestimating this parameter and thus exploring an upper limit to flux injected into the heliosphere (although the model does not account for closed flux added by very small-scale transients [e.g., *Moldwin et al.*, 2000]). However, no flux catastrophe is seen to occur for IFO times ~50 days, as the flux returns to the baseline value at each solar minimum. These long flux opening timescales mean that a small fraction of the ICME flux could remain closed when the leading edge reaches the heliopause, but the extreme length of these closed loops means they can essentially be considered open (see discussion below of electron signatures on very long closed field lines), though still contributing to the total heliospheric flux.

[21] Our simulation results demonstrate that CMEs alone can cause the observed solar cycle variation in magnetic flux, which could have implications for a range of helio-

spheric phenomena (e.g., galactic cosmic ray modulation by transients [*Newkirk et al.*, 1981; *Gopalswamy*, 2004]). This view contrasts with the conclusions of *Richardson et al.* [2002] and *Wang et al.* [2000a]. The contrasting views are easily reconciled, however, by recognizing that because the closed ICME flux in our model extends far out in the heliosphere, it would be treated as open by *Richardson et al.* [2002] and *Wang et al.* [2000a]. *Richardson et al.* [2002] identify ICME flux by in situ signatures which are likely to fade when the leading edge of an ICME lies well beyond the spacecraft location, as discussed further below. *Wang et al.* [2000a] treat as open any field line loops that extend beyond their model source surface, which lies well sunward of any spacecraft observing the solar cycle variation of flux. If that variation is due solely to ICMEs, as we propose, there is no need to postulate some unknown open-field source. In the model of *Wang et al.* [2000b], the open-field source is emerging bipolar active regions. These are likely proxies for CMEs (which the model cannot accommodate) and thus may be consistent with ICMEs as the source of the solar cycle variation of magnetic flux. Consistent with this view, *Luhmann et al.* [1998, 1999] demonstrated that newly opened magnetic flux between successive potential field solutions to the coronal magnetic field corresponds well with the time and location of observed CMEs.

[22] In the simulations we noted features (such as the Gnevyshev gap and the lag between the CME rate and $|\mathbf{B_{1AU}}|$ peaks) that may be better explained by longer IFO times coupled with a reduced estimate for the typical ICME flux content. However, to fully constrain such estimates requires detailed simulations over a long time period. This is difficult to achieve since continuous, intercalibrated observations of CME rates are only available over a single solar cycle.

[23] In order to convert the total heliospheric flux content to a quantity suitable for comparison with observations (i.e., $|\mathbf{B_{1AU}}|$), it is necessary to assume the radial component of the magnetic field intensity is constant over a sphere at 1 AU, which is supported by observations [*Smith and Balogh*, 2003]. Additionally, we note the lack of a latitudinal dependence of the CME distribution in the simulation. As the time scales for the flux variations are large, it is assumed that a heliospheric equilibrium is reached so as to remove any latitudinal effects (i.e., the extra CME flux close to the ecliptic compresses the high-latitude ambient open flux). However, such assumptions need to be tested with more sophisticated simulations and comparisons to observations.

[24] Finally, we note one set of observations that do not immediately fit with the long IFO time model. *Pagel et al.* [2005] recently showed that suprathermal electron signatures of disconnection appear to be rare, where disconnection is reconnection between two open field lines that releases a U-shaped field line with no connection to the Sun. While our model assumes that interchange reconnection with ICME loops (Figure 1), not disconnection elsewhere, is the process that reduces heliospheric flux, the suprathermal electron signature of this interchange reconnection may well look like disconnection for long IFO times. If interchange reconnection occurs when the apex of an ICME loop is far from the Sun, it is unlikely to carry the counterstreaming electron signature that signals connection to the Sun at both ends, an argument used in

section 1 to explain why closed ICME flux would be treated as open by *Richardson et al.* [2002]. The sunward electron beam will probably disappear owing to scattering along the lengthy path it must travel to reach the observing spacecraft situated much closer to the Sun. Without counterstreaming, the loop will appear to be open, and the signature of interchange reconnection will look like reconnection between two open fields, that is, like disconnection. In the study by *Pagel et al.* [2005], it is possible that disconnection signatures were not regularly seen because they occur on time scales shorter than the 10-min averaging interval used. A preliminary analysis suggests this may well be the case [*Crooker and Pagel*, 2005]. Further observations and theoretical efforts, however, are required to resolve this issue.

References

Brueckner, G. E., et al. (1995), The large angle spectroscopic coronagraph (LASCO), *Sol. Phys.*, *162*, 357.

Burlaga, L. F. (1988), Magnetic clouds: Constant alpha force-free configurations, *J. Geophys. Res.*, *93*, 7217.

Cargill, P. J., J. Chen, D. S. Spicer, and S. T. Zalesak (1996), Magnetohydrodynamic simulations of the motion of magnetic flux tubes through a magnetised plasma, *J. Geophys. Res.*, *101*, 4855.

Crooker, N. U., and C. Pagel (2005), Disconnection signatures of field line opening in ICME legs, *EOS Trans. AGU*, *86*(52), Fall Meet. Suppl., Abstract SH13A-0299.

Crooker, N. U., J. T. Gosling, and S. W. Kahler (1998), Magnetic clouds at sector boundaries, *J. Geophys. Res.*, *103*, 301.

Crooker, N. U., J. T. Gosling, and S. W. Kahler (2002), Reducing heliospheric flux from coronal mass ejections without disconnection, *J. Geophys. Res.*, *107*(A2), 1028, doi:10.1029/2001JA000236.

Crooker, N. U., R. Forsyth, A. Rees, J. T. Gosling, and S. W. Kahler (2004), Counterstreaming electrons in magnetic clouds near 5 AU, *J. Geophys. Res.*, *109*, A06110, doi:10.1029/2004JA010426.

Gnevyshev, M. N. (1977), Essential features of the 11 year solar cycle, *Sol. Phys.*, *51*, 175.

Gopalswamy, N. (2004), A global picture of CMEs in the inner heliosphere, in *The Sun and the Heliosphere As an Integrated System*, *ASSL Ser.*, edited by G. Poletto and S. Suess, pp. 201–251, Springer, New York.

Gosling, J. T., D. N. Baker, S. J. Bame, W. C. Feldman, and R. D. Zwickl (1987), Bidirectional solar wind electron heat flux events, *J. Geophys. Res.*, *92*, 8519–8535.

Lockwood, M., R. J. Forsyth, A. Balogh, and D. J. McComas (2004), Open solar flux estimates from near-Earth measurements of the interplanetary magnetic field: Comparison of the first two perihelion passes of the Ulysses spacecraft, *Ann. Geophys.*, *22*, 1395–1405, Sref-ID:1432-0576/ag/2004-22-1395.

Luhmann, J. G., J. T. Gosling, J. T. Hoeksmam, and X. Zhao (1998), The relationship between large-scale magnetic field evolution and coronal mass ejections, *J. Geophys. Res.*, *103*, 6585–6593.

Luhmann, J. G., J. T. Gosling, J. T. Hoeksama, X.-P. Zhao, N. Arge, and O. C. St. Cyr (1999), Connections between the slow solar wind, CMEs, and the helmet streamer belt inferred from coronal field models, in *Solar Wind Nine*, edited by S. R. Habbal et al., *AIP Conf. Proc.*, *471*, 725–728.

Lynch, B. J., J. R. Gruesbeck, T. H. Zurbuchen, and S. K. Antiochos (2005), Solar cycle-dependent helicity transport by magnetic clouds, *J. Geophys. Res.*, *110*, A08107, doi:10.1029/2005JA011137.

McComas, D. J., J. T. Gosling, and J. L. Phillips (1992), Interplanetary magnetic flux: Measurement and balance, *J. Geophys. Res.*, *97*, 171–177.

Moldwin, M. B., S. Ford, R. Lepping, J. Slavin, and A. Szabo (2000), Small-scale magnetic flux ropes in the solar wind, *Geophys. Res. Lett.*, *27*, 57–60.

Newkirk, G., Jr., A. J. Hundhausen, and V. Pizzo (1981), Solar cycle modulation of galactic cosmic rays: Speculation on the role of coronal transients, *J. Geophys. Res.*, *86*, 5387–5396.

Owens, M. J., V. G. Merkin, and P. Riley (2006), A kinematically distorted flux rope model for magnetic clouds, *J. Geophys. Res.*, *111*, A03104, doi:10.1029/2005JA011460.

Pagel, C., N. U. Crooker, D. E. Larson, S. W. Kahler, and M. J. Owens (2005), Understanding electron heat flux signatures in the solar wind, *J. Geophys. Res.*, *110*, A01103, doi:10.1029/2004JA010767.

Reinard, A. A., and L. A. Fisk (2004), Reconnection of magnetic field lines near the solar surface during coronal mass ejection propagation, *Astrophys. J.*, *608*, 533–539.

Richardson, I. G., H. V. Cane, and E. W. Cliver (2002), Sources of geomagnetic activity during nearly three solar cycles (1972–2000), *J. Geophys. Res.*, *107*(A8), 1187, doi:10.1029/2001JA000504.

Riley, P., and N. U. Crooker (2004), Kinematic treatment of CME evolution in the solar wind, *Astrophys. J.*, *600*, 1035–1042.

Riley, P., J. T. Gosling, and N. U. Crooker (2004), *Ulysses* observations of the magnetic connectivity between coronal mass ejections and the Sun, *Astrophys. J.*, *608*, 1100–1105.

Shodhan, S., N. U. Crooker, S. W. Kahler, R. J. Fitzenreiter, D. E. Larson, R. P. Lepping, G. L. Siscoe, and J. T. Gosling (2000), Counterstreaming electrons in magnetic clouds, *J. Geophys. Res.*, *105*, 27,261–27,268.

Smith, E. J., and A. Balogh (2003), Open magnetic flux: Variation with latitude and solar cycle, in *Solar Wind Ten*, edited by M. Velli, R. Bruno, and F. Malara, *AIP Conf. Proc.*, *679*, 67–70.

Wang, Y.-M., J. Lean, and N. R. Sheeley Jr. (2000a), The long-term variation of the Sun's open magnetic flux, *Geophys. Res. Lett.*, *27*, 505–508.

Wang, Y.-M., N. R. Sheeley Jr., and J. Lean (2000b), Understanding the evolution of the Sun's open magnetic flux, *Geophys. Res. Lett.*, *27*, 621–624.

Webb, D. F., R. P. Lepping, L. F. Burlaga, C. E. DeForest, D. E. Larson, S. F. Martin, S. P. Plunkett, and D. M. Rust (2000), The origin and development of the May 1997 magnetic cloud, *J. Geophys. Res.*, *105*, 27,251–27,259.

Yashiro, S., N. Gopalswamy, G. Michalek, O. C. St. Cyr, S. P. Plunkett, N. B. Rich, and R. A. Howard (2004), A catalog of white light coronal mass ejections observed by the SOHO spacecraft, *J. Geophys. Res.*, *109*, A07105, doi:10.1029/2003JA010282.

Yashiro, S., N. Gopalswamy, S. Akiyama, G. Michalek, and R. A. Howard (2005), Visibility of coronal mass ejections as a function of flare location and intensity, *J. Geophys. Res.*, *110*, A12S05, doi:10.1029/2005JA011151.

_____

N. U. Crooker and M. J. Owens, Center for Space Physics, Boston University, Boston, MA 02215, USA. (mjowens@bu.edu)